Journal of Magnetic Resonance 208 (2011) 235–242

Contents lists available at ScienceDirect

Journal of Magnetic Resonance

journal homepage: www.elsevier.com/locate/jmr

One-dimensional scanning of moisture in heated porous building materials with NMR

G.H.A. van der Heijden *, H.P. Huinink, L. Pel, K. Kopinga

Department of Applied Physics, Transport in Permeable Media, Eindhoven University of Technology, P.O. Box 513, 5600 MB Eindhoven, The Netherlands

ARTICLE INFO

Article history:
Received 6 August 2010
Revised 26 October 2010
Available online 17 November 2010

Keywords:
MRI
Non-isothermal
Moisture transport
Concrete

ABSTRACT

In this paper we present a new dedicated NMR setup which is capable of measuring one-dimensional moisture profiles in heated porous materials. The setup, which is placed in the bore of a 1.5 T whole-body scanner, is capable of reaching temperatures up to 500 °C. Moisture and temperature profiles can be measured quasi simultaneously with a typical time resolution of 2–5 min.

A methodology is introduced for correcting temperature effects on NMR measurements at these elevated temperatures. The corrections are based on the Curie law for paramagnetism and the observed temperature dependence of the relaxation mechanisms occurring in porous materials. Both these corrections are used to obtain a moisture content profile from the raw NMR signal profile.

To illustrate the methodology, a one-sided heating experiment of concrete with a moisture content in equilibrium with 97% RH is presented. This kind of heating experiment is of particular interest in the research on fire spalling of concrete, since it directly reveals the moisture and heat transport occurring inside the concrete. The obtained moisture profiles reveal a moisture peak building up behind the boiling front, resulting in a saturated layer. To our knowledge the direct proof of the formation of a moisture peak and subsequent moisture clogging has not been reported before.

1. Introduction

The presence of water in building materials plays an important role in many damage processes. Especially the two phase changes of water, freezing and boiling, can lead to damage. On the other hand, salts that are present in building materials may cause damage if water is present to dissolve and transport them [1,2].

An extreme example of moisture related damage to a building material is fire spalling of concrete. If a fire occurs in a concrete tunnel or building, the surface of a concrete wall is heated to temperatures well above 100 °C within minutes, rising up to 1200 °C. Moisture in the concrete will start to boil and the water vapour can only escape via the heated surface. Because concrete is a very low permeable material, high vapour pressures may be generated. A combination of these high vapour pressures, thermal stresses resulting from large temperature gradients, and weakening of the porous matrix due to dehydration can cause the concrete to spall (delaminate) [3]. Under extreme conditions it can even give rise to explosive spalling.

In fire spalling of concrete moisture and heat transport at high temperatures play an important role. Both these transport processes take place inside a building material. Combined measurements of moisture content and temperature inside a material, as a function of position and time, are essential to understand the process but are difficult to obtain. It has been demonstrated that with NMR it is possible to measure the moisture content in a building material in a quantitative way [4,6,7].

In this paper we present a new dedicated NMR setup which is capable of measuring both moisture content and temperature profiles during extreme one-sided heating of porous materials such as concrete, fired-clay brick, wood, and gypsum. These measurements give a unique insight in the physical processes in for instance fire spalling of concrete. During a one-sided heating experiment the moisture content changes rapidly and a large temperature gradient is present in the sample. Interpretation of the NMR signal profiles is not straightforward since this temperature gradient will influence the measured signal profiles. Furthermore, in order to obtain a satisfactory temporal resolution the used NMR pulse sequence is limited in its duration. We will present a measurement and correction method by which quantitative moisture profiles can be obtained. We will use an experiment on a concrete sample to demonstrate this method.

In Section 2 the NMR setup and the materials and methods will be introduced, and the theory behind non-isothermal NMR will be discussed. In Section 3 the result of a concrete fire spalling experiment and the used signal corrections will be presented. Finally, in Section 4 the concluding remarks will be given.

* Corresponding author. Fax: +31 402432598.
E-mail address: l.pel@tue.nl (G.H.A. van der Heijden).

1090-7807/$ - see front matter © 2010 Elsevier Inc. All rights reserved.
doi:10.1016/j.jmr.2010.11.010

2. Non-isothermal NMR experiments

2.1. NMR setup

The fire spalling experiments were performed using a home-built NMR setup, which was especially designed for non-isothermal moisture measurements on building materials. A schematic diagram of this setup is shown in Fig. 1. The setup can be placed entirely in the bore of a 1.5 T whole-body medical scanner (Gyroscan, Philips), which is used only for its main magnetic field. Two coils, in an anti-Helmholtz configuration, with a diameter of 35 cm, provide a constant magnetic field gradient G in the direction of B_0. The magnitude of the gradient is 100 mT m^{-1}, providing a spatial resolution of about 4–5 mm with the used pulse sequences.

A home built birdcage coil (12 legs, low-pass configuration) is used for sending the RF pulses (B_1) and receiving the NMR signal from the sample. The coil is made from copper strips wrapped around an aluminium oxide (Al_2O_3) tube. The coil is 140 mm long and has a diameter of 140 mm. A birdcage type coil is used because it generates a homogeneous B_1 field perpendicular to the long axis of the cylindrical sample. Therefore, the coil can be placed parallel to the main magnetic field, providing optimal use of the available space inside the bore. The coil is designed with an internal Faraday shield, in order to prevent changes in the dielectric constant of the sample from de-tuning the RF coil [4]. In this way, quantitative moisture content measurements can be performed.

The Al_2O_3 tube can withstand temperatures far above the requirements of the experiments (melting temperature 2072 °C). Furthermore, it does not give any background signal, which is important when measuring a moisture content as low as 0.03 m^3 m^{-3} in concrete at high temperatures. Two trimming capacitors (specified voltage of 12 kV) were used for tuning and matching. In order to ensure a constant resonance frequency and sensitivity of the coil, capacitors with a high thermal stability were used.

A high power RF amplifier (3.6 kW, 63.9 MHz) is used in order to achieve the relative short RF pulses (~50 μs) needed for NMR measurements on concrete. The Faraday cage placed around the coil has a twofold purpose: it shields the NMR coil from spurious RF signals and it prevents the RF pulses from reaching the electronic systems of the medical scanner.

In order to simulate the conditions as occur in a fire, the concrete has to be heated up quickly. With an array of four 100 W halogen lamps, capable of generating a heat flux of 12 kW m^{-2}, we are able to mimic a 'fire' inside the NMR setup. The reflectors of the lamps are gold plated to ensure maximum reflection of infrared radiation towards the sample surface. To minimise heating of the RF coil, the lamp array is cooled. The heat flux from the lamp was calibrated calorimetrically and varies linearly with the applied electrical power to the lamp [8]. The maximum temperature which can be reached at the heated surface is about 400–500 °C. Although we do not reach the maximum temperatures occurring in a real life fire (~1000 °C), we are in the region of temperatures where the most interesting moisture related processes occur, such as boiling at temperatures higher than 100 ° C, moisture clogging, and dehydration of the concrete.

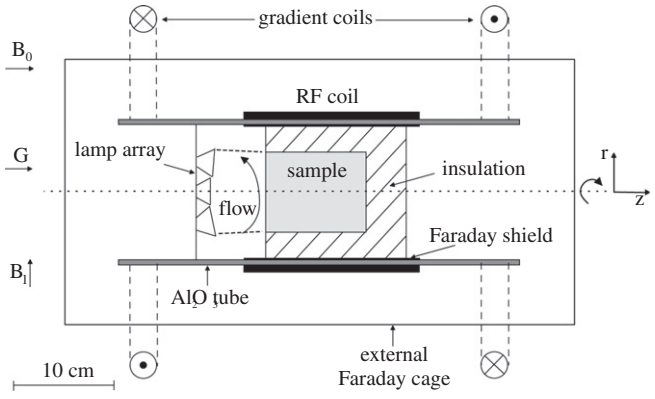

Fig. 1. Schematic diagram of the NMR setup. A whole-body 1.5 T MRI scanner generates the main magnetic field B_0. Two coils in an anti-Helmholtz configuration provide a constant magnetic field gradient G of 100 mT m^{-1}. A bird-cage RF coil with a diameter of 140 mm is used for both sending the RF pulses and receiving the NMR signal. The bird-cage coil is constructed on an aluminium oxide (Al_2O_3) tube. An array of four 100 W halogen lamps is used to heat the sample, which is thermally insulated and positioned in the bird-cage coil.

The temperatures inside the sample were measured using type-K thermocouples. The thermocouples were found to slightly decrease the signal to noise ratio of the measurements. At the receiving end of the thermocouple wires a low-pass filter is used to minimise the RF signal at the inputs of the thermocouple amplifier.

2.1.1. Pulse sequence

To obtain a full moisture profile of the sample a so-called 'multi frequency scan' was used. Slice selection is achieved with a constant magnetic gradient. A solid echo ($90_y - \tau - 90_x - \tau$ – echo) is used to obtain the signal of at each selected frequency. The frequencies are scanned in an interleaved manner in order to minimise the measurement time [5]. The bandwidth of the coil (~400 kHz) is large enough to scan the entire sample without moving it. To obtain a complete one-dimensional signal profile, the NMR signals measured at different frequencies/positions are combined. In order to obtain a good temporal resolution the complete NMR signal decay cannot be measured at each point of the profile, but is only determined at a suitably chosen position.

2.1.2. Sample preparation

The concrete sample is pressed in a PTFE holder to seal all sides except for the heated surface (transverse plane of the cylinder). In this way the moisture transport is limited to one dimension. PTFE was used because it does not contain hydrogen. A major drawback of PTFE is that toxic fumes can be released when it is heated above 300 °C. Therefore, a ventilation system is used to extract smoke or fumes produced in the setup during the experiment. The flow of heat is limited to one dimension by insulating the sample using mineral wool, at the same time preventing the RF coil from heating. From numerical analysis of the heat conduction of the setup geometry and the materials used, the radial temperature gradient is estimated to be 5–10% of the longitudinal temperature gradient. By creating a one dimensional moisture and heat transport experiment, the conditions inside a concrete wall are simulated.

At the start of the experiment one moisture and temperature profile is measured to record the initial state of the sample. The first moisture profile (homogeneous moisture content) is used to correct subsequent profiles for the longitudinal inhomogeneity of the RF field. Next the heating is turned on and the moisture and temperature profiles are measured every 2–5 min, depending on the number of averages needed to obtain a satisfactory signal to noise ratio.

2.2. Concrete characterisation

Concrete is a porous material with pore-sizes ranging from only a few nanometers to several microns [9]. The pores can be subdivided in gel pores (2–10 nm), capillary pores (10–200 nm), and cracks or air voids (>1 μm). The degree of saturation of this pore system will depend on the relative humidity (RH). At 40% RH the gel pore system is saturated and above this RH the capillary pores will start to fill. At 100% RH the cracks are also filled with water and the material is fully saturated. The water which is found in

the pore system is called evaporable or free water, which is defined as water removed by drying at 105 °C. However, a significant amount of water is chemically bound to the cement paste by the hydration reaction. The chemically bound water is released from the concrete at temperatures ranging from 105 °C to 500 °C by a reaction called dehydration.

All water in the concrete, either free or chemically bound, will contribute to the NMR signal. However, a wide range in mobilities of the water molecules is found in concrete, which will result in a wide range of relaxation times. The relaxation time of chemically bound water in concrete is about 20 μs [10]. The signal decay of free water inside concrete ranges from 100 μs to about 40 ms. The NMR signal decay obtained from a saturated concrete sample will therefore contain a wide range of relaxation times T_2 corresponding to the different pore systems:

$$S(t) = \sum_i A_i \exp\left(-\frac{t}{T_{2,i}}\right), \quad (1)$$

where A_i is the amplitude of the contribution of a pore sub system: chemically bound water, gel pores, capillary pores, and cracks/air voids.

In Fig. 2a relaxation time distributions are shown for the concrete (water cement ratio 0.5) which is used in the experiments. An Ostroff–Waugh sequence with an inter-echo time of 160 μs was used to measure the signal decay. The top curve corresponds to a capillary saturated concrete. The regions of the different components are indicated by the dashed lines. The three main contributions to the signal are water in the gel, capillary pores, and air voids or micro-cracks (>1 μm). The arrow indicates the progression of the drying. It can be seen that the longer T_2 components decrease in amplitude first, which is to be expected since the largest pores in the material are emptied first. Note that the gel pores are dominant in terms of signal contribution. In the saturated concrete, the capillary pores contribute 8% to the total signal, which decreases to zero at a temperature of 105 °C. The fact that the gel pores are dominating the NMR signal is also important in determining the first order correction parameters which will be discussed in the next section.

The NMR signal was calibrated with respect to the total moisture content in the concrete. To this end the sample was initially capillary saturated. Mass and NMR signal were recorded simultaneously while the sample was dried slowly at room temperature. The signal is shown as a function of the normalised mass (m/m_0) in Fig. 2b. Where m_0 is the mass of a capillary saturated concrete sample. The normalised mass is used because in this way both evaporable and chemically bound water can be depicted on the same axis. For temperatures up to 105 °C the NMR signal at an echo time t_e is proportional to the amount of evaporable moisture present in the concrete. This is indicated by the linear fit (solid line) of the NMR signal vs. moisture content in the range of 1–0.94.

After drying at a constant temperature of 105 °C a signal $S \lesssim 0.1$ was measured. The signal must be originating from chemically bound water in the concrete. The NMR signal was also calibrated with respect to amount of chemically bound water at temperatures above 105 °C (see inset in Fig. 2b). To this end the sample was dried at several temperatures until a constant mass was obtained. Note that the NMR signal was measured after the sample was cooled down to room temperature under a 0% RH atmosphere. In this way, no moisture was absorbed during cooling and the moisture content reached at a certain temperature is preserved.

The NMR signal decreased for temperatures from 105 °C to 130 ° C (see inset graph). The decrease in signal is caused by a decrease of water which is strongly absorbed in pores with sizes of only a few nanometers (smallest gel pores) which will boil/evaporate at temperatures up to 130 °C.

The mass loss in the temperature range of 130–250 °C indicates that the chemically bound moisture content of the concrete decreases. However, the signal remains constant (see inset graph), which indicates that the water lost in this temperature range is not contributing to the NMR signal. When the temperature is further increased from 250 °C to 500 °C more water is lost and the signal decreases to zero. Although the relaxation time (~20 μs) is much shorter than the inter-echo time, the signal to noise ratio was sufficient to obtain a signal. If the concrete is fully hydrated the amount of chemically bound water in the concrete mix is ~10% by mass. Furthermore, not all chemically bound water has the same relaxation time, and therefore does not contribute to the same extent to the signal at t_e. The relationship between signal and moisture content for temperatures above 105 °C is not linear. Therefore, it is not possible to obtain a degree of dehydration of the concrete from the measured signal.

2.3. Non-isothermal NMR

The NMR measurements described above were performed at room temperature. In our experiments the free moisture content is of interest and we have observed that the NMR signal can be calibrated with respect to the amount of free water. However, in a

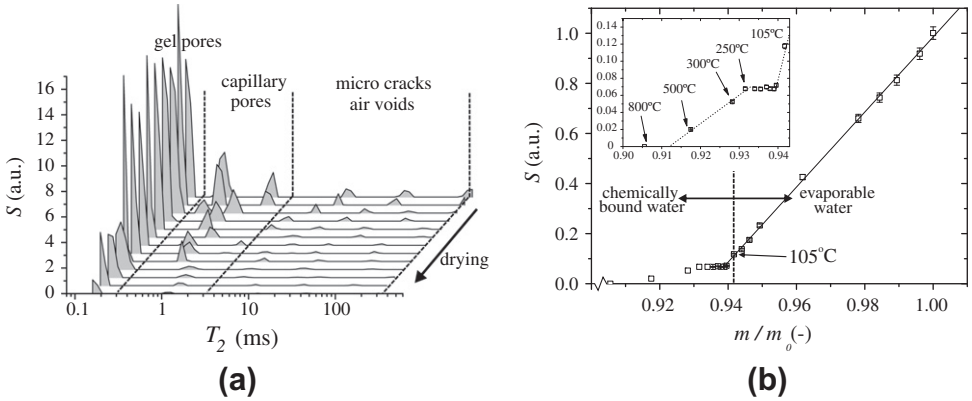

Fig. 2. Characterisation with NMR of the concrete sample for different moisture contents. (a) The relaxation time distributions (Contin inversion routine) obtained during drying of a saturated concrete. The signal decays were measured using an Ostroff–Waugh sequence. (b) A calibration of the NMR signal with respect to the amount of moisture present in the concrete. The NMR signal is plotted as a function of the normalised mass m/m_0. The NMR signal from the chemically bound moisture is obtained at room temperature and for a set of drying-temperatures from 105 to 800 °C (see inset). The amount of signal measured for temperatures from 130 °C to 250 °C is constant. At temperatures above 250 °C the signal decreases to zero. The background signal is in the order of 10^{-3}.

one-sided heating experiment the temperature will increases well above 100 °C and large temperature gradients will be present in the sample. Therefore, in the next section the theory is explained which will be used to correct the signal in order to obtain a quantitative moisture content.

2.3.1. Temperature dependent magnetisation

The nuclear magnetisation M of a material placed in an external magnetic field B_0 depends on the absolute temperature of the material [11]:

$$M(T) = \frac{n\mu\hbar\omega}{4kT},$$

where n is the number of nuclei, μ the magnetic moment of ^{1}H, $\hbar\omega$ the energy difference between the two possible energy states, k the Boltzmann constant, and T the absolute temperature.

The magnitude of the measured signal is not only determined by the nuclear magnetisation, but also by the relaxation times. Both spin–spin T_2 as spin–lattice T_1 relaxation are temperature dependent, and can cause a change in the observed signal [12]. The transverse magnetisation M_{xy} in a Hahn spin-echo experiment with a repetition time t_r and an echo time t_e is given by:

$$M_{xy}(t_e, t_r, T) = M_0(T)\exp\left(-\frac{t_e}{T_2(T)}\right)\left(1-\exp\left(-\frac{t_r}{T_1(T)}\right)\right), \quad (2)$$

provided that $T_1 \gg T_2$. The influence of the temperature on the transverse magnetisation can be analysed by taking the partial derivative with respect to temperature [12]:

$$\frac{\partial \ln M_{xy}(t_e, t_r, T)}{\partial T} = -\frac{1}{T} + \frac{t_e}{T_2^2}\frac{\partial T_2}{\partial T} - \frac{t_r}{T_1^2}\frac{\exp\left(-\frac{t_r}{T_1}\right)}{1-\exp\left(-\frac{t_r}{T_1}\right)}\frac{\partial T_1}{\partial T}. \quad (3)$$

In order to separate the different contributions to the temperature dependence, we have chosen to take the derivative of the logarithm of the magnetisation. The first term at the right hand side represents the inverse temperature dependence of the magnetisation. The second and third term represent the temperature dependence of T_2 and T_1, respectively. The magnitude of these terms is largely determined by the ratio between the experimental parameters t_r and t_e, and T_1 and T_2, respectively. In case of concrete $T_1 \sim 1$ ms. With a repetition time of 0.1 s, the temperature dependence of T_1 can be neglected. However, since the magnetisation thermalises exponentially with T_1, the approximation given above is only valid if the amount of heating in a typical time $t = T_1$ is small. In the following experiment the temperature increase in a time T_1 is about 10^{-3} °C.

However, depending on the porous material, we cannot always conduct our experiment in such a way that the influence of the temperature dependence of T_2 can be neglected. For example, in concrete the relaxation time of water in the gel pores is in the order of 200–400 μs. The echo time we use in our experiments is 160 μs. Consequently, any change in T_2 with temperature will be reflected in the magnitude of the measured signal. In the next section we will discuss the temperature dependence of the transverse relaxation time of water inside a porous material in more detail.

2.3.2. Temperature dependent relaxation

In a porous material, different dominant relaxation mechanisms can exist depending on the pore size, surface relaxivity, and chosen NMR parameters such as the field gradient and echo time. In the discussion of relaxation mechanisms of water in a porous material the focus will be on the transverse relaxation, since in these materials in general $T_1 \geqslant T_2$ and the influence of T_1 can minimised by using a sufficiently large long delay. Furthermore, we will only take into account the situation found in concrete where relaxation is dominated by surface relaxation.

2.3.2.1. Surface relaxation. In bulk water, the water molecules experience no restrictions in their movement. However, water molecules in a porous material will spend a certain time in the vicinity of the pore wall. The chance of relaxing is higher close to the surface. This can be either due to a susceptibility mismatch between water and the porous material, due to the presence of paramagnetic ions at the surface, or due to crystal defects in the surface, resulting in the presence of unpaired electron spins (especially in oxides) [13].

Depending on the pore-size distribution of the material, different surface relaxation regimes can be identified. Consider the case in which there is a fast exchange in the timescale of the experiment (t_e) between water close to the surface and the centre of a pore, which is the so-called fast diffusion regime. In this regime the relaxation rate is given by [14]:

$$\frac{1}{T_{2,S}} = \frac{1}{T_{2,B}} + \rho_2\frac{S}{V}, \quad (4)$$

where ρ_2 is the surface relaxivity, S/V is the surface to volume ratio of the pore, and $T_{2,B}$ the bulk relaxation time which can be neglected because for water $T_{2,B} \gg T_{2,S}$. If the surface relaxivity is known, the relaxation times measured by NMR can be used to calculate the surface to volume ratio of a porous material. By assuming a certain pore size geometry, e.g. cylindrical or spherical, one can obtain a pore-size distribution.

The temperature dependent factor in the fast diffusion regime is the surface relaxivity. Without going into the details of the chemical composition of the surface, one can describe the temperature influence on the surface relaxivity by an Arrhenius type equation [15]:

$$\rho_2(T) = \rho_{2,0}\exp\left(\frac{\Delta E}{RT}\right), \quad (5)$$

where $\rho_{2,0}$ is the surface relaxivity at a certain reference temperature and ΔE is the effective surface interaction energy. The effective interaction energy is a combination of the energies involved in surface diffusion and surface relaxation, respectively. It must be noted that this type of description is purely phenomenological and that the temperature dependence of the surface relaxivity depends strongly on the chemical composition of the surface.

3. Results

To demonstrate the capabilities of the NMR setup and to show how the temperature influences the NMR measurements we will give an example of a one-sided heating experiment of concrete. First we will present the uncorrected 'raw' signal profiles. Next, we will discuss the corrections which will be applied to obtain the quantitative moisture content.

3.1. Signal profiles

The concrete sample used in the experiment was equilibrated at an RH of 97%, corresponding to a moisture content of 0.07 $m^3\,m^{-3}$. The sample is heated with a heat flux of 12 kW m^{-2}. The measured signal and temperature profiles are shown in Fig. 3. In this figure, the heated surface is located at 0 mm, and the back of the sample is at 100 mm. No corrections for the temperature dependence of magnetisation or relaxation have been applied. However, the signal profiles are normalised with respect to the initial signal profile S_0. At the start of the experiment the moisture is homogeneously distributed throughout the sample ($S/S_0 = 1$). The profiles were

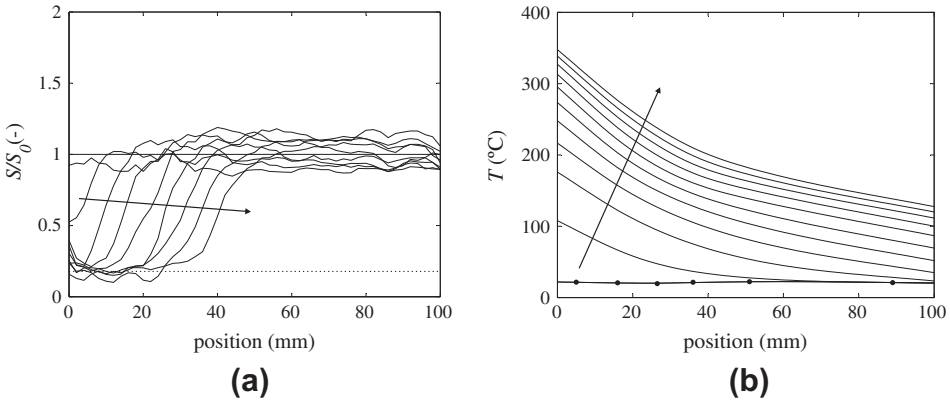

Fig. 3. (a) Uncorrected signal (S) profiles as a function of the position inside the concrete. The profiles are shown for every 8.5 min. The arrows in the figures indicate the progress in time. The heated surface corresponds to x = 0 mm and the back of the sample to x = 100 mm. The profiles have been normalised with respect to the first profile (S_0), but have not been corrected for temperature. The initial moisture content of 0.07 $m^3\ m^{-3}$ corresponds to S/S_0 = 1. (b) Time evolution of the temperature profiles, the positions of the thermocouples are indicated by black dots.

measured every 4.2 min, but for clarity only one out of every two profiles is shown.

In the signal profiles a clear front is observed, which indicates that liquid water is evaporated. Furthermore, it can be seen that the signal behind the front increases 10% above the initial signal level, which is unexpected when drying.

In the region close to the surface (0–30 mm) the signal does not decrease to zero and a background check with an empty coil revealed no signal. The temperature in this region is 250–350 °C. Therefore, this signal has to originate from the chemically bound water in the cement paste (see Fig. 2b).

After 20 minutes, the temperature at the surface is 200 °C, whereas the back of the sample is still at 20 °C. The signal profiles cannot be directly interpreted as moisture profiles, due to the large temperature differences between the start of the experiment. Furthermore, a large temperature gradient is present in the sample. In the next section we will discuss the necessary temperature corrections for concrete.

3.2. Signal correction

The temperature dependence of the nuclear magnetisation is given by Eq. (2). The correction of the inverse temperature dependence is straightforward since all the signal can be re-scaled by $1/T$. Therefore we will focus on the temperature dependence of the relaxation times and the influence on the measured signal.

3.2.1. Relaxation correction

In the NMR signal decay obtained from saturated concrete given by Eq. (1) the temperature dependence can be introduced:

$$S(t,T) = \sum_i A_i(T) \exp\left(-\frac{t}{T_{2,i}(T)}\right). \tag{6}$$

In concrete there are three dominant relaxation time contributions. The temperature dependence of the these relaxation times are shown as Arrhenius plots in Fig. 4. We have included gypsum for comparison since in gypsum only one pore size (~1 μm) is found, whereas in concrete multiple pore-sizes are present. The relaxation times were obtained from a multi-exponential fit of the signal decay curves. As already shown in Section 2.2, for concrete the signal decay can be described by three exponents which can be related to the three pore systems. It can be seen from Fig. 4 that in all three pore systems the relaxation time increases with temperature. The surface relaxivity therefore decreases with temperature. However, the energy corresponding to the surface interactions is different for each of the pore systems. These activation energies are listed in Table 1. We can see that as the pore size decreases the effective energy decreases.

The relaxation times $T_{2,i}$ all have a different temperature dependence. Therefore, each pore system which is contributing to the total signal should be corrected separately. To obtain a quantitative moisture content θ a temperature and pore system dependent correction factor $c_i(T)$ is applied:

$$\theta = \sum_i c_i(T) A_i(T) \exp\left(-\frac{t_e}{T_{2,i}(T)}\right). \tag{7}$$

Note that we have written this equation for $t = t_e$ because this is the time at which the signal is recorded. The correction factor c_i contains both the magnetisation correction as well as the exponential relaxation time correction factor. A full correction of the signal should include a relaxation correction for all three relaxation times with temperature. Consequently, during the experiment at each degree of saturation and temperature the distribution of the moisture over the three pore systems needs to be known.

The overall influence of the relaxation correction for a particular pore system i on the total signal depends firstly on the amplitude of the relaxation time contribution and secondly on the ratio t_e/T_2. We have seen in Section 2.2 that the maximum contribution of the capillary pores and the micro-cracks to the total signal was about 10%. Furthermore, the ratio t_e/T_2 is 5×10^{-2} for the capillary pores and 3×10^{-3} for the micro-cracks. This already indicates that the influence of the temperature dependence for these two pore systems is negligible. Therefore, in case of concrete for t_e = 160 μs correction of only the gel pores is sufficient.

To illustrate this we have plotted in Fig. 5a the correction factor c_i as a function of temperature. Three different corrections are shown: the correction for the nuclear magnetisation (solid line), the total correction including relaxation for the gel pores, and the total correction for the capillary pores.

In case of the gel pores the relaxation time correction results in a significantly different correction factor of about half of the initial correction. Note that the total correction of the gel pores is effectively smaller since the relaxation time correction for the gel pores is larger than one. For the capillary pores, this correction at 100 °C amounts to 1%, which is negligible. We have excluded the relaxation time correction for the micro-cracks from the discussion since the correction factor will coincide with the solid line.

During heating of the concrete the amplitudes of the different pore systems will decrease due to drying. It is observed that the relaxation time corresponding to the gel pores does not signifi-

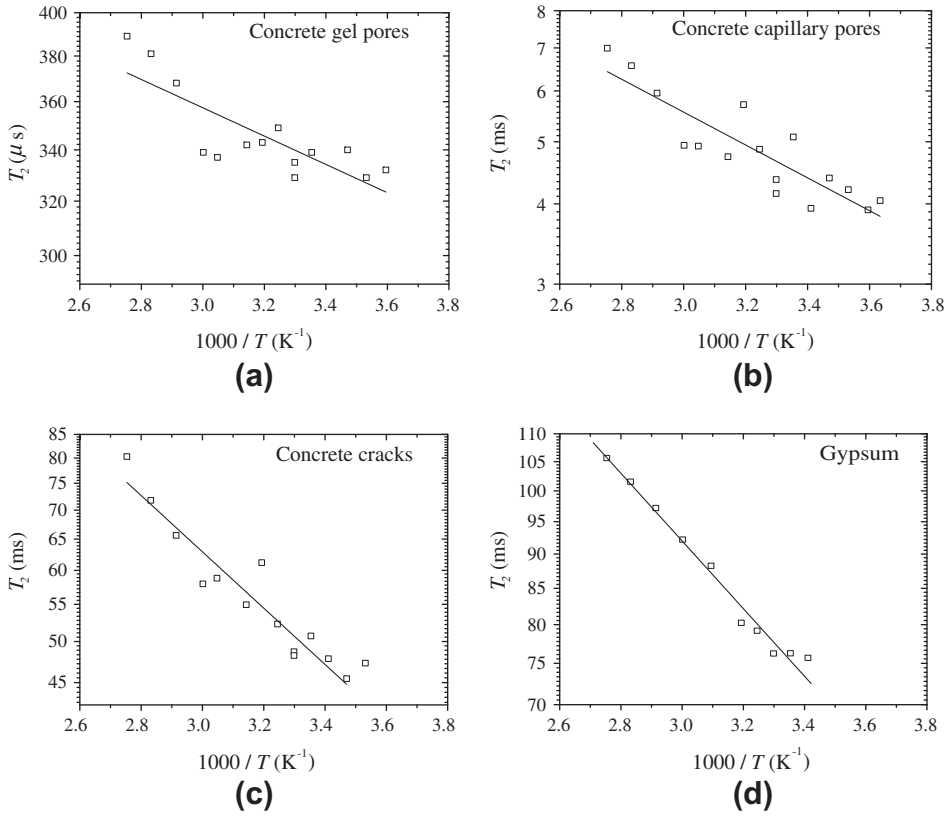

Fig. 4. Arrhenius plots of the transverse relaxation time. From the top left to bottom right: relaxation times of water in gel pores, capillary pores, concrete cracks, and gypsum. The solid lines are fits of a straight line to the data.

Table 1
Measured activation energy for transverse relaxation of water in gel pores, capillary pores, and cracks of concrete. For comparison gypsum is also included.

Porous material	Energy (kJ mol^{-1})
Concrete (gel)	1.8
Concrete (capillary)	4.4
Concrete (cracks)	5.6
Gypsum	4.3

cantly change during emptying of the gel pores. Furthermore, as can be seen in the signal profiles the transition from signal to no signal is sharp. Any relaxation time dependence of the signal will not significantly change the signal profiles in this region.

3.3. Fire spalling experiment

We will now take one of the signal profiles from Fig. 3 and apply both the magnetisation as well as the total correction including relaxation of the gel pores. The influence of both corrections is shown in Fig. 5b. Here, the uncorrected signal profile (solid line), the magnetisation corrected (M, dash-dotted line), and the total corrected (M + R, dashed line) are shown. The magnetisation correction increases the measured signal at a position of 40 mm from 1.1 to 1.6. Although the temperature, and thus correction, is higher close to the surface, no significant change of the moisture profile upon correction (correction indicated by bold curve Fig. 5a). The dashed line shows the result after both magnetisation and relaxation correction. The more or less homogenous signal profile from 40 to 100 mm shows a distinct peak at 40 mm after the correction.

The complete set of corrected signal profiles (see Fig. 6) can be used to get a better understanding of the physics behind the moisture transport processes taking place in concrete. In this figure we show both the corrected signal profiles (a) as well as the measured temperature profiles (b) already shown in Fig. 3b. Four observations regarding the moisture profiles can be made. Firstly, immediately after the heating is started, a boiling front enters the sample. The temperature at the boiling front rises from 150 °C to 195 °C. From the temperature measured at the boiling front we can estimate the saturated vapour pressure to be ~1.3 MPa. This pressure is of the same order of magnitude as was measured in a similar heating experiment in concrete directly by means of a pressure transducer [16]. These pressures are close to the typical tensile strength of concrete, which is about 3–5 MPa.

Secondly, because of the high vapour pressure at the boiling front, vapour can be convected in two directions, towards the surface, and towards the back of the sample. The vapour flux towards the surface flows into a region of higher temperatures. The vapour flux in the opposite direction flows into a region of lower temperatures. Hence, this part of the vapour condenses and the moisture content increases and forms a moisture peak. Note that condensation takes place at a temperature of about 140 °C (see □ in Fig. 6b). These temperatures were measured at the peak in moisture content.

Thirdly, the moisture peak increases and even reaches saturation behind the boiling front. The saturated layer widens and due to the limited size of the sample (100 mm) the back of the sample also becomes saturated. The maximum moisture content reached in this experiment corresponds to the saturated moisture content of the concrete. Without proper correction one would not have come to this conclusion (see uncorrected signal profiles).

Fourthly, a saturated porous material has a capillary pressure close to zero and as a consequence the vapour pressure at the boiling front can become comparable to or larger than the capillary

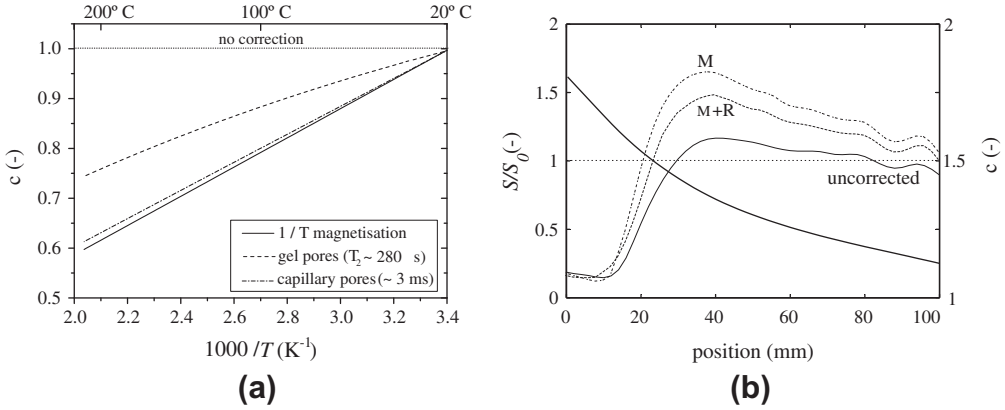

Fig. 5. (a) The first three contributions to the overall temperature correction as a function of temperature. The temperature correction factor for the nuclear magnetisation ($1/T$, solid line). The extra contribution of the surface relaxation for the concrete gel pores (dashed line). The extra contribution of the capillary pores (dash-dotted line). (b) Corrections applied to the raw signal profile in concrete after 42 min (solid line). The signal profile which is corrected for the temperature dependence of the magnetisation is indicated by M. The moisture profile which is corrected the temperature dependence of both magnetisation and relaxation is indicated by M + R. The total correction factor is shown by the bold curve.

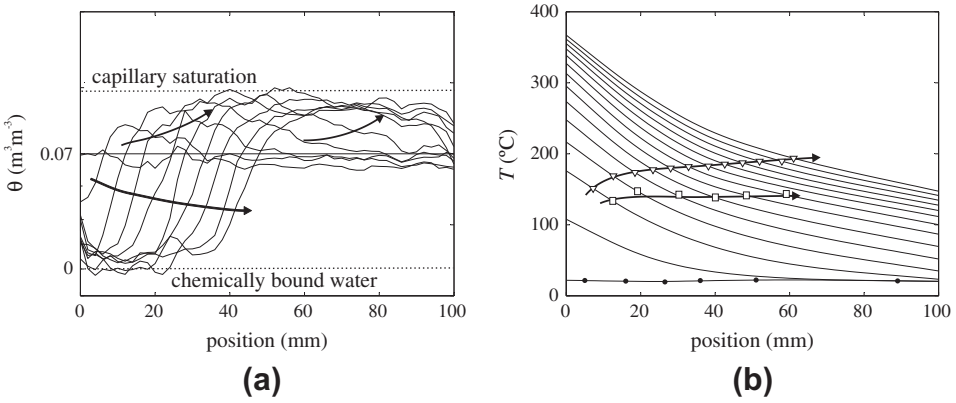

Fig. 6. (a) Corrected moisture profiles and (b) temperature profiles. As the temperature increases quickly to above 100 °C a boiling front develops. The temperature at the front is marked in the temperature profiles (▽). The dashed line indicates the 100 °C isotherm. As the boiling front progresses a moisture peak develops. This peak increases and reaches saturation after 30 min. The temperatures at the moisture peak are indicated in the temperature profiles (□). The temperature at the surface increases to about 350 °C. The profiles are shown every 8.5 min. The arrows in the figures indicated the progress in time.

pressure. It can possibly generate a liquid water flow towards the back of the sample. In practice it is observed that a concrete wall will start to 'bleed' water from larger cracks at the cold side. Note that the vapour cannot be transported through a saturated layer of concrete because the relative vapour permeability is zero. The speed at which the moisture content at the back side of the sample increases indicates that possibly liquid moisture is pushed back by the increased vapour pressure. However, no direct evidence for this process is available.

4. Conclusions

We have presented a new NMR setup which makes it possible to measure non-isothermal moisture transport in a variety of building materials. Realistic temperature gradients, mimicking that of a fire, can be applied. Simultaneous measurements of moisture and temperature yield valuable information on the physical mechanisms behind damage processes. Up till now, the existence of a moisture peak and the development of a saturated region was only predicted by models. To our knowledge this measurement is the first direct quantitative evidence for this process.

As we have shown, temperature measurements are essential in these non-isothermal experiments, as they provide the proper correction needed to obtain accurate quantitative moisture profiles. It must be noted that the proper correction factor may be different for different porous materials. Therefore, for each porous material a calibration of the NMR signal with temperature is needed.

Acknowledgments

This research was supported by the Dutch Technology Foundation (STW, Grant 07045). We would like to thank Jef Noijen and Hans Dalderop for their help in constructing the NMR setup and gold coating of the halogen lamps.

References

[1] G.W. Scherer, Crystallization in pores, Cement and Concrete Research 29 (8) (1999) 1347–1358.
[2] G.A. Khoury, Effect of fire on concrete and concrete structures, Progress in Structural Engineering and Materials 2 (2000) 429–447.
[3] F.A. Ali, D. O'Connor, A. Abu-Tair, Explosive spalling of high-strength concrete columns in fire, Magazine of Concrete Research 53 (3) (2001) 197–204.
[4] K. Kopinga, L. Pel, One-dimensional scanning of moisture in porous materials with nmr, Review of Scientific Instruments 65 (12) (1994) 3673–3681.
[5] M.T. Vlaardingerbroek, J.A. den Boer, Magnetic Resonance Imaging, 3rd ed., Springer Verlag, 2003.
[6] L. Pel, K. Kopinga, H. Brocken, Determination of moisture profiles in porous building materials by nmr., Magnetic Resonance Imaging 14 (7–8) (1996) 931–932.

[7] L. Pel, H. Brocken, K. Kopinga, Determination of moisture diffusivity in porous media using moisture concentration profiles, International Journal of Heat and Mass Transfer 39 (6) (1996) 1273–1280.
[8] G.H.A. van der Heijden, H.P. Huinink, L. Pel, K. Kopinga, Non-isothermal drying of fired-clay brick, an nmr study, Chemical Engineering Science 64 (12) (2009) 3010–3018.
[9] T.C. Hansen, Physical structure of hardened cement paste. A classical approach, Materials and Structures 19 (114) (1986) 423–436.
[10] J.Y. Jehng, D.T. Sprague, W.P. Halperin, Pore structure of hydrating cement paste by magnetic resonance relaxation analysis and freezing, Magnetic Resonance Imaging 14 (7–8) (1996) 785–791.
[11] C.P. Slichter, Principles of Magnetic Resonance, Springer Verlag, Berlin, 1989.
[12] D.H. Gultekin, J.C. Gore, Temperature dependence of nuclear magnetization and relaxation, Journal of Magnetic Resonance 172 (1) (2005) 133–141.
[13] R.L. Kleinberg, Nuclear magnetic resonance, in: Po-Zen Wong (Ed.), Methods in the Physics of Porous Media, Experimental Methods in the Physical Sciences, 35th ed., Elsevier, 1999, pp. 337–385 (Chapter 9).
[14] K.R. Brownstein, C.E. Tarr, Importance of classical diffusion in nmr studies of water in biological cells, Physical Review A 19 (6) (1979) 2446.
[15] S. Godefroy, M. Fleury, F. Deflandre, J.P. Korb, Temperature effect on nmr surface relaxation in rocks for well logging applications, The Journal of Physical Chemistry B 106 (43) (2002) 11183–11190.
[16] P. Kalifa, F.D. Menneteau, D. Quenard, Spalling and pore pressure in hpc at high temperatures, Cement and Concrete Research 30 (12) (2000) 1915–1927.